Macromolecules 1994, *27*, 5–11

Multiphase Materials with Lignin. 11. Starlike Copolymers with Caprolactone

Willer de Oliveira and Wolfgang G. Glasser*

Department of Wood Science and Forest Products, and Biobased Materials Center, Virginia Polytechnic Institute & State University, Blacksburg, Virginia 24061-0323

Received April 14, 1993; Revised Manuscript Received September 24, 1993®

ABSTRACT: Multiphase starlike copolymers have been prepared using polycaprolactone as hard, arm segments and hydroxypropyl lignin as the core of the star. Copolymer architecture differed in terms of the average number of arms per core, which ranged between 2 and 7; and in terms of hydroxypropyl lignin molecular size and T_g, which ranged between 2100 and 6400 D and -7 and +85 °C, respectively. The copolymers, which had nearly uniform but broad molecular weight distributions, were analyzed with regard to solution properties, thermal characteristics, and crystallinity. The Mark–Houwink–Sakurada exponential factor remained virtually constant (i.e., ca. 0.66) for all copolymer types. The thermal characteristics were all in support of multiphase morphology, and they differed with copolymer architecture. Copolymers having hydroxypropyl lignin with T_g's greater than the T_m of caprolactone resulted in significant T_m depression, whereas this could not be observed for copolymers with low T_g cores. T_m increased with arm length as the degree of polymerization of the caprolactone rose to 50. Crystallinity was established for all copolymers, even those with arms shorter than 10 caprolactone units in length.

Introduction

Multiphase block copolymers with thermoplastic processability have been the subject of extensive interest due to their useful engineering properties. With the exception of cellulose,[1,2] few examples in the literature have dealt with the use of natural polymers as thermoplastic elastomers. In previous research, lignin has been successfully used as an active component in synthetic polymers.[3] It was seen that through chemical alkoxylation, starlike telechelic polyols having rigid aromatic lignin centers and multiple flexible polyether arms could be obtained. This type of lignin-derived telechelic polyol has been used in the synthesis of thermosets or as a segment for thermoplastic materials.[3–8] Thus in light of the importance of morphological features of multiphase block copolymers, and considering the success of preparing lignin-based telechelic polyols, we have attempted to examine the synthesis and properties of a multiphase lignin-containing macromolecular system with thermoplastic processability. It was expected that an appropriate selection of segments to be attached to, or copolymerized with, lignin-derived telechelic polyols would yield multiphase copolymers with useful properties, thereby opening new avenues for lignin utilization.

Poly(ϵ-caprolactone) (PCL) and its copolymers have attracted much attention because of their favorable miscibility characteristics, their biodegradability, their ability to disperse pigments, and their low-temperature adhesiveness.[9] A–B–A terpolymers in which the A blocks comprise linear polylactone units have been used as plasticizers for poly(vinyl chloride) resins and additives in tape joint compounds with improved drying characteristics.[10] Block terpolymers of styrene, butadiene, and ϵ-caprolactone have been prepared with properties typical of thermoplastic elastomers.[11] Triblock poly(propylene oxide)–polycaprolactone copolymers with rubbery–crystalline–rubbery multiphase morphology were also synthesized.[12]

Due to the attractive features of polycaprolactone segments, and owing to the reactivity of its monomer with polyols to form copolymers, it was the objective of this study to synthesize and examine the solution- and solid-state behavior of multiphase block copolymers based on PCL and lignin-derived telechelic polyols such as hydroxypropyl lignin (HPL). Design parameters included compositional variables on both sides, the PCL arm component and the HPL core component. In addition, block dimensions and method of synthesis were to be examined in relation to copolymer morphology and properties.

Experimental Section

Materials and Methods. Softwood kraft lignin (Indulin AT, Westvaco Corporation, North Charleston, SC) served as starting material for the synthesis of HPL, in accordance with earlier work.[13,14] HPL was purified by either liquid–liquid extraction or by fractional precipitation in a manner described elsewhere.[15] Some lignin derivatives were modified by reaction with diethyl sulfate so as to reduce overall OH functionality. This procedure has been described previously.[4]

Poly(ϵ-caprolactone) prepolymers monohydroxy-terminated (PCL) with number average molecular weights of 4400 and 11300 D were purchased from Scientific Polymer Products, Inc., Ontario, NY.

ϵ-Caprolactone (CL) was obtained from Aldrich Chemical Company. It was distilled over ground calcium hydroxide prior to use. 2,4-Tolylene diisocyante (TDI) and stannous octanoate were obtained from Aldrich Chemical Company and Sigma Co., respectively, and used without further purification. Tetrahydrofuran (THF) was supplied by Fisher Scientific Chemical Company. The solvent was dried over a mixture of metallic potassium and benzophenone. This mixture was refluxed and distilled under dry nitrogen. THF was stored over molecular sieves.

Anionic Copolymerization with CL Monomer. In a typical reaction, a calculated amount of dried HPL and stannous octanoate was charged into the flask and flushed with prepurified and dried nitrogen. A calculated amount of CL (previously distilled) was then syringed into the flask and the mixture stirred until a homogeneous solution resulted. The mixture was heated to 100–110 °C for approximately 15 h after which the temperature was raised to 150–160 °C for an additional 5–10 h.[16] Following cooling, the reaction product was dissolved in THF and precipitated into methanol or aqueous methanol, filtered, extracted in a Soxhlet apparatus to remove unreacted HPL, and dried under vacuum.

---

* To whom correspondence should be sent.

® Abstract published in *Advance ACS Abstracts*, November 15, 1993.

0024-9297/94/2227-0005$04.50/0

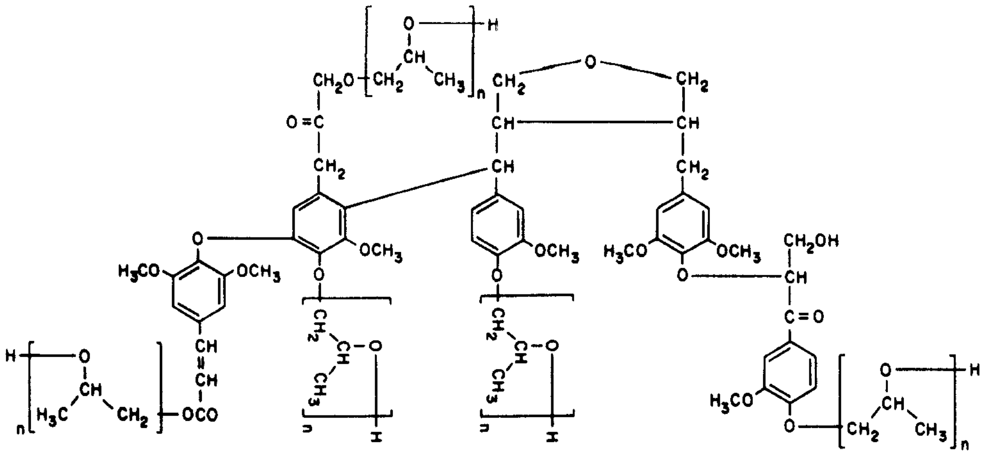

Figure 1. Schematic representation of hydroxypropyl (organosolv) lignin derivative (n = 1).[4]

Table 1. Properties of Hydroxypropyl Lignin

samples	M_n	M_w	M_w/M_n	OH (%)	OH^a/M_n	T_g (°C)	lignin (wt %)	PO^c (wt %)
$HPL_{2.1}$	2100	10000	4.8	5.7	7.0	85	83	17
$HPL_{6.4}$	6400	67900	10.6	1.0	3.5^b	-7	27	73
$HPL_{3.5}$	3500	20300	5.8	3.0	7.0	1	50	50

[a] Number of hydroxyl equivalents per molecular weight. [b] Following capping by reaction with diethyl sulfate. [c] Propylene oxide content.

Grafting with PCL Segments. Copolymers were also prepared by reacting monoisocyanate-terminated PCL prepolymer with HPL in dry THF using stannous octanoate as catalyst.[17] The monoisocyanate-terminated prepolymer segments were prepared by reacting the OH-terminated PCL with TDI in THF at 50 °C. Stannous octanoate served as catalyst, and the TDI and PCL molar ratio was approximately 5:1. After several hours the product was isolated by precipitation into petroleum ether, filtered, washed (petroleum ether), and dried. The monoisocyanate-capped prepolymer was used immediately. IR spectroscopy was used to monitor the reaction.[18] The grafting reaction proceeded at 50 °C over 24 h under rigorously anhydrous conditions. The copolymer was isolated by precipitation into aqueous methanol.

Spectroscopic Characterization. FTIR spectra were recorded using a Nicolet 5SX spectrophotometer; samples were prepared by dispersion in KBr. UV spectra were recorded in chloroform solution using a Varian/Cary-219 UV-VIS spectrophotometer. These methods were used for the analysis of NCO functionality and lignin content, respectively.

Gel Permeation Chromatography (GPC). The molecular parameters (molecular weight, Mark–Houwink–Sakurada constants, and intrinsic viscosity) of the copolymers were determined by GPC with a differential viscosity detector and a differential refractive index (concentration) detector (Waters 410) in sequence.[19-22] THF served as mobile phase. Polystyrene standards were used for the construction of the universal calibration curve. The intrinsic viscosity is measured as a function of retention volume by combining the viscosity chromatogram from the differential viscometer with the concentration chromatogram from a refractive index detector. The calculations were performed by UNICAL software on a IBM-compatible computer.

Differential Scanning Calorimetry (DSC). DSC (Perkin-Elmer Series 7) thermograms were obtained using a standard aluminum pan. Nitrogen was used as a sweeping gas, and the heating rate was 10 °C/min. Glass transition temperatures were taken as midpoints of the change in slope of the baseline, and T_m was taken as the temperature corresponding to endothermic peak location. Crystallinity was calculated according to the following equation:

$$X_c(\%) = (\Delta H_f/\Delta H_f^*) \times 100$$

where ΔH_f is the measured heat of fusion for the sample, and ΔH_f^* is the heat of fusion for 100% crystalline CL.[23]

Optical Microscopy. Optical microscopy was conducted on a Zeiss Axioplan polarizing optical photomicroscope fitted with a LinKam TMS 90 Hot Stage and a Zeiss ML 100 camera. Nucleation and growth behavior of the copolymers were observed on thin films of copolymers between glass plates.

Results and Discussion

I. Synthesis. The branched HPL core that serves as centerpiece of the starlike copolymers may represent a variety of design features. Optional cores have different lignin content, different molecular weight and weight distribution, different T_g (by virtue of chain extension with propylene oxide), and a variable number of hydroxyl groups (i.e., hydroxyl content). Typically, non-sulfonated lignins are obtained with number-average molecular weights ranging between 10^3 and 10^4, and with dispersities between 2 and 20.[24] Although lignin, in nature, serves as hard segment, having a glass transition temperature between 90 and 180 °C,[3,6,24] lignin can be easily converted into a soft segment by alkoxylation.[7] Following hydroxypropylation, hydroxypropyl–lignin derivatives are telechelic polyols with uniform functionality (i.e., aliphatic OH; Figure 1). Selection of parent lignin and degree of chain extension with propylene oxide, primarily, dictate the properties of the core of the starlike copolymer.

The HPL used in this study (Table 1) represented three different types that (a) were either "soft" or "hard" at room temperature, as dictated by their glass transition temperatures (T_g) being above (hard) or below (soft) room temperature; (b) had lignin contents between 27 and 83% by weight; (c) had molecular weights between M_n 2100 and 6400 D; and (d) had hydroxyl contents between 1 and 5.7%. The latter corresponds to a functionality (i.e., the number of hydroxyl groups per number average molecular fragment) of between 3.5 and 7.

Starlike copolymers of HPL and PCL may be synthesized by anionic polymerization of ε-caprolactone on the hydroxyl end group of HPL (Figure 2) or by a grafting process of monofunctional isocyanate terminated PCL onto HPL (Figure 3). The growing of arms by copolymerizing CL with HPL may be performed using standard anionic polymerization conditions and a catalyst.[16] Whereas the number of arms is determined on the basis of the average number of hydroxyls of HPL, the length of arms is dictated by degree of chain extension with CL (i.e., stoichiometry). When both methods of synthesis are

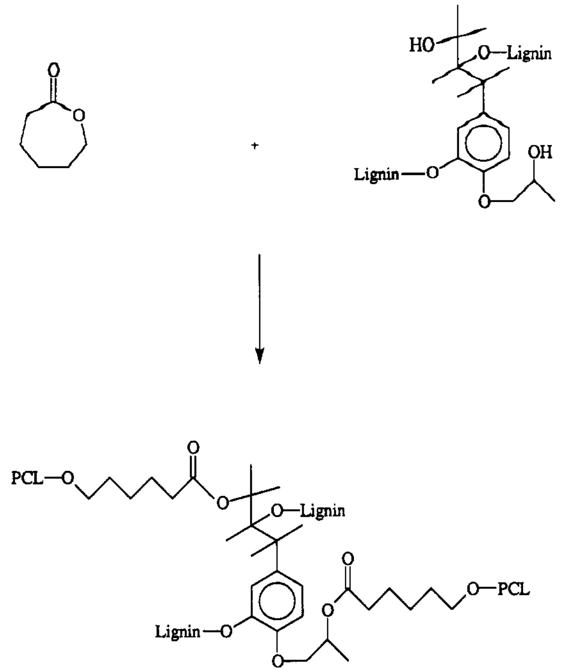

Figure 2. Schematic synthesis route for the preparation of HPL–PCL starlike copolymers via anionic polymerization of ε-caprolactone monomers onto hydroxypropyl lignin.

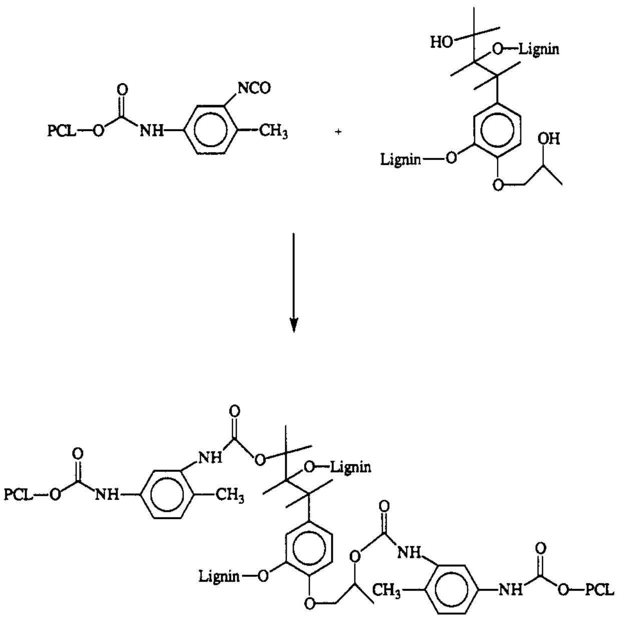

Figure 3. Schematic synthesis route for the preparation of HPL–PCL starlike copolymers via grafting of NCO-capped PCL preformed segments onto hydroxypropyl lignin.

compared in terms of molecular weight distribution (MWD), it is seen that copolymers with high HPL content have high MWD, independent of the method of synthesis. GPC chromatograms illustrate both cases in Figure 4. As the copolymer weight increases as a consequence of increasing arm length, a substantial decrease in the polydispersity of the copolymer is observed. This can be explained by the broad MWD of the starting HPL, since the arm length of the copolymer in both methods of synthesis should be statistically of narrow polydispersity. Despite the advantages (although costly) of fractionation of the HPL to generate copolymers with low polydispersity,[15] no fractionation of the starting material was attempted in this work.

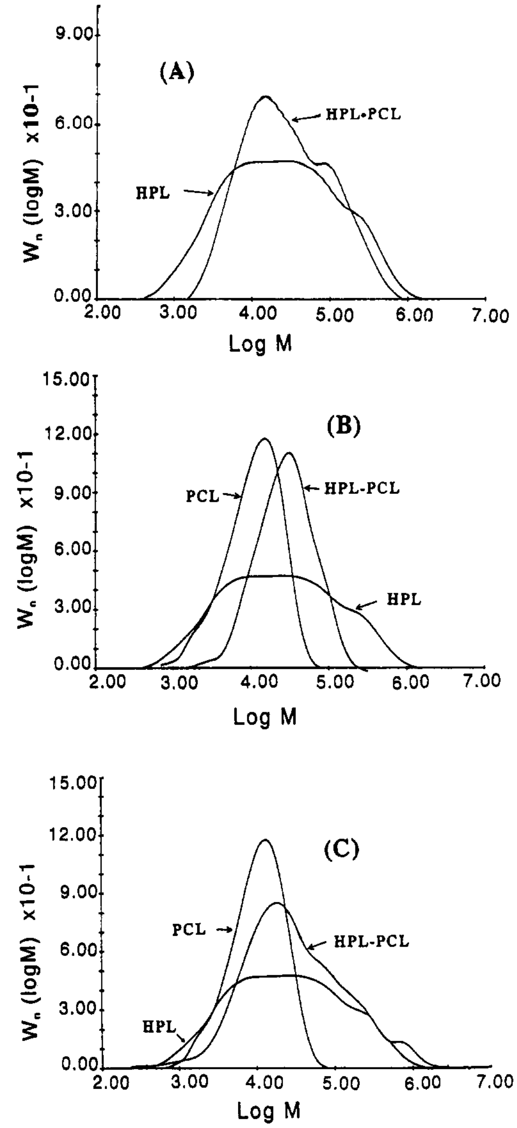

Figure 4. Typical molecular weight distribution of HPL–PCL starlike copolymers (and their corresponding prepolymers) synthesized (A) via anionic polymerization of ε-caprolactone monomer onto HPL and (B and C) via grafting of NCO-capped PCL preformed segments. Both B and C differ in composition. The former has a high PCL content, whereas the latter has a high HPL content.

Table 2. HPL-PCL Starlike Copolymer Samples

average no. of arms per core	average arm length (10^{-3} M_n) for core options[a]		
	$HPL_{2.1}$[a]	$HPL_{3.5}$[a]	$HPL_{6.4}$[a]
2–4 (variable)[b]		4.4 (2)[d] 11.3 (2)[d]	4.4 (1)[d]
3.5 (fixed)[c]			0.85–4.9 (7)[d]
7 (fixed)[c]	0.25–7.2 (8)[d]		

[a] Optical HPL cores classified according to M_n ($\times10^{-3}$) in subscript, i.e., $HPL_{2.1}$ signifies HPL core with M_n of 2100 Da. [b] Variable number of arms per core signifies attachment of preformed arms (at two available lengths, 4400 and 11300 Da) in variable number. [c] Fixed number of arms per core signifies attachment of arms by copolymerization (at variable arm extension) to a fixed number of reactive sites. [d] Number of samples prepared in each category in parentheses.

A total of 20 starlike block copolymers were synthesized in this study. These copolymers represented species that were obtained either by copolymerization or by the grafting of preformed arms. On this basis, it is possible to distinguish five different categories of starlike copolymers (Table 2). In all instances the copolymers were of overall larger molecular weight and of narrower molecular weight distribution, than the core HPL. Whether the final product reflected more closely the parent PCL or HPL

Table 3. Solution and Thermal Properties of HPL–PCL Starlike Copolymers

	solution properties[a]		thermal properties[b]					
copolymer type	IV (dL g^{-1})	*a*	$T_m{}^c$ (°C)	$T_m{}^d$ (°C)	$\Delta H_f{}^c$ (J g^{-1})	$\Delta H_f{}^d$ (J g^{-1})	$X_c{}^c$ (%)	$X_c{}^d$ (%)
$HPL_{2.1}$	0.056	0.195						
$HPL_{3.1}$	0.057	0.159						
$HPL_{6.4}$	0.104	0.243						
$PCL_{4.4}$	0.315	0.630	68	55	265	175	60	59
$PCL_{11.3}$	0.320	0.649	70	57	258	179	60	60
$HPL_{2.1}/7F_{0.24-7.2}{}^e$	0.11–0.31	0.63–0.67	45–59	27–48	24–159	25–133	5–36	9–44
$HPL_{3.5}/2-4V_{4.4}$	0.41–0.46	0.66	63–66	57	188–225	111–140	32–43	37–47
$HPL_{3.5}/2-4V_{11.3}$	0.45–0.51	0.59	62–65	57	157–233	113–163	36–53	38–54
$HPL_{6.4}/2-4V_{4.4}$	0.41	0.67	63		225	140	32	47
$HPL_{6.4}/3.5F_{0.85-4.9}$	0.14–0.39	0.64–0.66	52–63	39–58	102–210	95–150	23–48	32–50

[a] IV represents intrinsic viscosity; and a stands for the Mark–Houwink–Sakurada exponential factor. [b] T_m, ΔH_f, and X_c represent melting point, heat of fusion, and degree of crystallinity, respectively. [c] First heating. [d] Second heating. [e] Designations F and V represent fixed or variable number of arms per core (see Table 2). The subscript of F or V represents the average arm length (10^{-3} M_n); and the number before F or V (as in 7F or 2–4V) indicates the average number of arms per core.

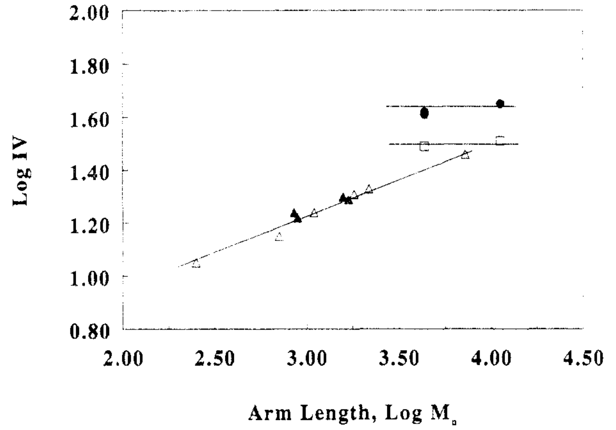

Figure 5. Relationship between intrinsic viscosity and copolymer arm length for HPL–PCL starlike copolymers synthesized by anionic polymerization (△, ▲) and by grafting of PCL preformed segments (●). Key: (△) copolymers from the series $HPL_{2.1}/7F$; (▲) series $HPL_{6.4}/3.5F$; (●) series $HPL_{3.5}/2-4V$ or $HPL_{6.4}/2-4V$, and (□) PCL homopolymer.

depended primarily on the weight fraction of either in the copolymer.

II. Solution Properties. The intrinsic viscosity and Mark–Houwink–Sakurada (MHS) exponential factor data from gel permeation chromatography (Table 3) reveal a virtually constant value of around 0.66 for the MHS exponent, a, for all block copolymers. Degree of branching, polydispersity, and method of synthesis have apparently no effect on the MHS constant. Both starlike copolymer and homopolymer (PCL) had almost identical MHS constants.

On the other hand the intrinsic viscosities are dependent on arm length, but not on the overall degree of branching (i.e., number of arms) (Table 3). The intrinsic viscosity varies with molecular weight when the average arm length increases (Figure 5). The rate of increase is the same for all copolymer types. Even when the average arm length is nearly as long as that of the parent linear polymer, the viscosities of the starlike polymers are still below that of the linear polymer of equivalent arm length (Figure 5). Thus, the presence of arms with short or intermediate sizes has the effect of reducing the intrinsic viscosity below the value that should be expected for linear polymers with equivalent molecular weights. For copolymers constructed using preformed arm segments at fixed arm length, the surprising result is that the overall intrinsic viscosity is greater than that of the linear PCL prepolymer that gave rise to the starlike copolymers. A possible explanation for this behavior involves the incorporation of a foreign group at the end of the PCL prepolymer, as the result of end-group capping with diisocyanate. It has been recognized, on the basis of experimental evidence, that terminal (polar) groups can affect the solution properties of polymers.[25] This has been demonstrated especially for polystyrene where the incorporation of hydroxy end groups was claimed to produce hydrophilically associated complexes in hydrocarbon solvents. The incorporation of even a small segment of a co-monomer into the polymer chain can alter the solution behavior of the polymer as observed in polystyrene–polydiene star block copolymers. According to Bi and Fetters,[26] this type of behavior is not predicted by theory, nor has it been observed for star materials containing homopolymer arms. It seems that these unexpected results are related to the incompatibility of the segments.

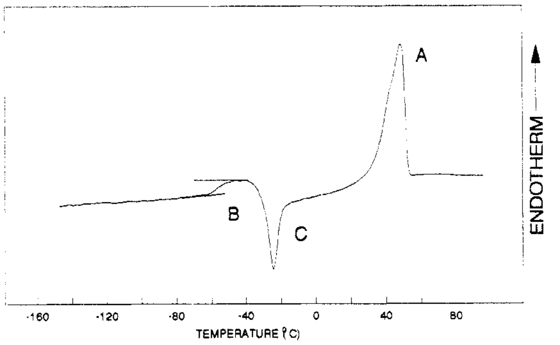

Figure 6. Typical DSC curve of copolymer for the series $HPL_{2.1}/7F$ quenched from the melt, where A, B, and C are the melting, glass, and crystallization temperatures, respectively. Heating rate is 10 °C/min.

In the absence of further experimental evidence, especially that based on concentrated solution viscosity measurements, the unexpected rise in intrinsic viscosity of the starlike copolymers with preformed arms over their linear PCL segments can tentatively be attributed to the incorporation of polar urethane-type linkages. The difference between the two methods of synthesis (i.e., copolymerization and arm attachment) suggests that the effect of urethane groups on the intrinsic viscosity in THF may be larger than that of branching.

III. Thermal Properties. A typical DSC thermogram for a selected $HPL_{2.1}/7F$ block copolymer, obtained in a second heating mode after quenching from the melt (Figure 6) reveals three major transitions: a first-order endothermic transition, A, at about 60 °C, which corresponds to the crystalline fusion of the PCL segment; a second-order transition, B, at −57 °C that corresponds to the T_g of PCL; and an exothermic peak, C, at about −25 °C which is due to the crystallization of PCL segments. The glass transition of the HPL core could not be detected by DSC

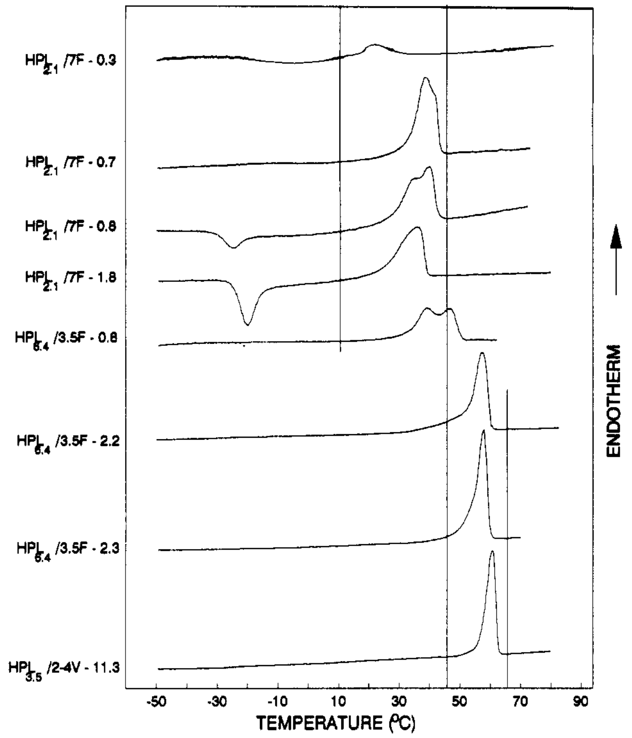

Figure 7. DSC curves for samples showing effects of block size (arm length of PCL segments) and composition, as well as the effect of T_g of the core (HPL) when it is above (HPL$_{2.1}$) or below (HPL$_{3.5}$ or HPL$_{6.4}$) the T_m of PCL segments.

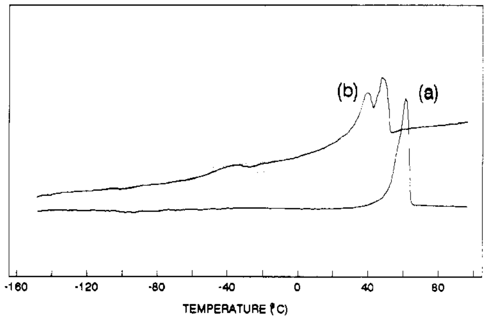

Figure 8. Typical DSC curves of copolymers from series HPL$_{3.5}$ or HPL$_{6.4}$: (a) first heating and (b) second heating quenched from the melt. Heating rate is 10 °C/min.

in this particular sample. This is explained with both the low molecular weight of HPL and its high T_g (approximately 85 °C) that is too close to the melting point of PCL arms to be distinguished with certainty. These two factors combined make the HPL glass transition temperature hard to detect. The main information derived from DSC measurements (Table 3) shows that there is a distinct difference in thermal behavior between the various copolymer types. (In the entire HPL$_{2.1}$/7F series, the T_g of the HPL phase could not be detected because of the proximity of the glass transition temperature of HPL to the T_m of PCL.) The DSC results for the copolymers of series HPL$_{2.1}$/7F and HPL$_{6.4}$/3.5F (Figure 7) exhibit crystallinity as supported by the presence of a melting endotherm even for samples which contain less that 50 wt % PCL for the copolymers having a core with T_g above the T_m of PCL. The T_g of PCL ranges from −49 to −57 °C (not shown). Upon heating the quenched samples, the PCL segments crystallize revealing a crystallization exotherm between −30 and −10 °C. The thermograms of copolymers having an HPL T_g below the T_m of PCL (i.e., the HPL$_{6.4}$/3.5F series) also indicate two major transitions. A first-order transition at about 60 °C accounts for the melting point of PCL; and a very broad, second-order transition, in the range of −75 to −20 °C corresponds to the glass transition of both amorphous HPL and PCL phases. Differently from the HPL$_{2.1}$/7F series, no crystallization exotherm is seen throughout the samples. This phenomenon will be discussed later. It is important to notice that the melting point of the PCL crystalline phase may be separated into two peaks, several degrees apart. The separation into two endotherms only occurs during the second heating (Figure 8). The thermogram of a copolymer annealed at room temperature for several months (Figure 8, curve a), reveals a single melting transition. The location of the T_g, however, is questionable. Very fast cooling of the melted copolymer maintained 3 min at 100 °C reveals, in the second heating (Figure 8, curve b), a very well defined T_g. This is located in between the glass transition temperature of the corresponding "homopolymers", HPL and PCL. The melting point is not only depressed by about 4–16 deg, but it is also split into two peaks. The presence of two melting points has been reported for several polymer systems,[27–32] including polycaprolactone.[27] Nylon-66 exhibits two endothermic melting peaks, which may be converted into one peak depending on the annealing conditions. The two peaks are due to the melting of two morphological species.[29] Thermal analysis of semicrystalline poly(aryl ether ether ketone) (PEEK) has shown double endothermic behavior due to different lamellar morphologies.[30–32] In the case of PCL, the data on multiple endothermic peaks are controversial. Huet and Marechal[27] have observed double endothermic peak formation after rapid cooling of PCL from the melt. This was interpreted with different crystalline morphologies of the polymer. A similar hypothesis was also formulated by Perret and Skoulios[28] on the basis of crystallization studies of PCL with different molecular weights. These hypotheses are, however, contradictory to the work of Chatani et al.[33] which has shown only one crystal structure for PCL. Therefore, the explanation of the double endothermic peak for PCL cannot be based on two different crystalline morphologies, as previously hypothesized. Instead, the double peak is most probably based on lamellar thickening (annealing) as a consequence of heating during thermal analysis. The observed double melting endotherm is the result of two different lamellar structures (different in thickness) created during the fast-cooling treatment. When enough time is allowed for crystallization to occur, both peaks merge into one peak (Figure 8, curve a) as a consequence of uniformity in the thickness of the lamellae.

The thermal behavior of all types of copolymers does not change significantly with molecular weight (Table 3). The melting point is the parameter which varies most with molecular weight. The relationship between T_m and PCL arm length (Figure 9) shows that the melting point approaches a limit of 60 °C as the molecular weight of the PCL arms increases. The data also show that the highest molecular weight copolymer from the HPL$_{2.1}$/7F series does not fit the curve. This is consistent with the earlier reported observation that copolymers from this series require more time to reach a thermal equilibrium and that this affects T_m. After aging (T_m of the first heating), the melting points of the high molecular weight copolymers migrate to a higher temperature (Table 3), in accordance with the pattern of Figure 8.

The crystallization of PCL chains is greatly affected by the T_g of the HPL core. In order to examine the morphology during the crystallization of PCL chains, thin films were heated while under observation by optical microscopy in polarized light. The optical micrographs of starlike copolymers from the HPL$_{2.1}$/7F series with varying PCL content and arm length, isothermally crys-

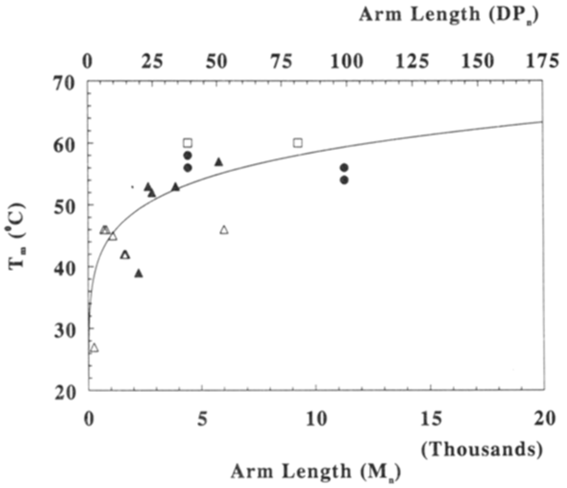

Figure 9. Relationship between melting point and copolymer arm length (second heating mode after quenching from the melt). Symbols are as in Figure 5.

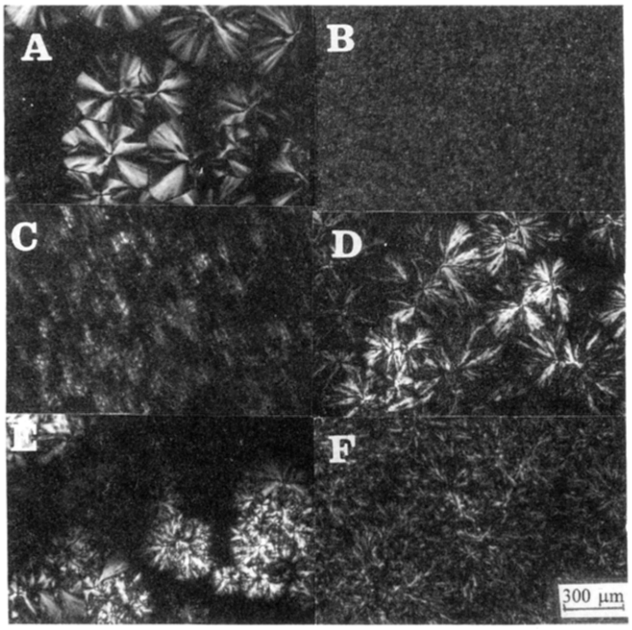

Figure 10. Optical micrographs of PCL and copolymers from the series $HPL_{2.1}$/7F where the T_g of the HPL is above the T_m of PCL segments: (A) 100% PCL, (B) 5% lignin, (C) 12% lignin, (D) 17% lignin, (E) 20% lignin, and (F) 28% lignin.

tallized from the melt (Figure 10), show that the samples exhibit spherulitic texture and that the shape of the spherulites changes as the concentration of amorphous HPL in the copolymer increases. The coarseness of the spherulites at high HPL content (Figure 10, parts E and F) is a consequence of covalent bonding between amorphous and crystalline blocks. Within the spherulites are both segments, amorphous HPL and crystalline PCL, chemically tied together by covalent bonds. Since they cannot macroscopically separate, the PCL chains still crystallize, but the shape of the spherulites is disturbed by the presence of amorphous material forced to remain within the spherulite.

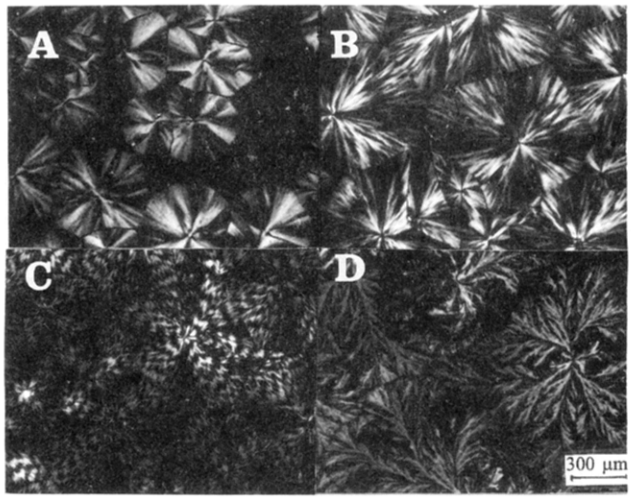

Figure 11. Optical micrographs of PCL and copolymers from the series of $HPL_{3.5}$ or $HPL_{6.4}$, where the T_g of HPL is below the T_m of PCL segments: (A) 100% PCL, (B) 6% lignin, (C) 15% lignin, and (D) 21% lignin.

Optical micrographs of copolymers from the $HPL_{3.5}$ and $HPL_{6.4}$ series, with decreasing PCL content, allow again the observation (Figure 11) that the irregularity of the spherulites increases as the copolymer becomes richer in amorphous HPL phase. However, a close inspection of the micrographs in Figure 10 reveals that $HPL_{2.1}$ series copolymers are much more irregular than the corresponding copolymers from other series. Even though it is true for all three series that the coarseness of the spherulites increases with HPL content, the spherulite shapes in the $HPL_{3.5}$ and $HPL_{6.4}$ series are almost identical to the homopolymer PCL. The presence of HPL does not prevent the formation of a well-defined spherulitic structure. This can be explained with the nature of the $HPL_{3.5}$ and $HPL_{6.4}$ copolymers. As reported previously, at the crystallization temperature of PCL chains, both HPL and PCL are in the rubbery state, above their T_g's. There is no restriction to chain mobility, and this helps both spherulite formation and the definition of contours. Similar observations have been reported in block copolymers of polystyrene–polycaprolactone and polybutadiene–polycaprolactone.[34] In the $HPL_{2.1}$ series, the nature of the HPL component is different. Its T_g is above the melting point of PCL arms, and this restricts chain movement during crystallization. As the PCL arms crystallize, the glassy phase of HPL tends to counteract the radial growth of crystalline fibrils into spherulites, and this results in much greater coarseness in the texture of the spherulites. It also seems as if the HPL solid phase, along with high molecular weight PCL chains, helps to increase the nucleation density, as seen in the optical micrograph of Figure 10. However, a more detailed crystallization kinetics study would be required to be definitive on this point. These results are consistent with the thermal properties discussed previously.

IV. Crystallinity. The heat of fusion data from DSC for PCL and the copolymers synthesized in this study (Table 3) can be interpreted in terms of crystallinity. Since the copolymers melt only about 30 °C above room temperature, the amount of crystallinity changes with time due to a continuous crystallization process at room temperature. Therefore, the data on degree of crystallinity are from the first heating treatment of samples that had been aged for at least 6 months at ambient temperature in a desiccator. Figure 12 shows the variation of crystallinity content as a function of arm length. The results indicate that the degree of crystallinity is not only related to composition, but also to the length of PCL arms. As the PCL arm lengths increase, their ability to crystallize also increases, and this reaches the level of PCL homopolymer at about DP 100.

Conclusions

Starlike multiphase copolymers can be produced by either copolymerizing ϵ-caprolactone in the presence of

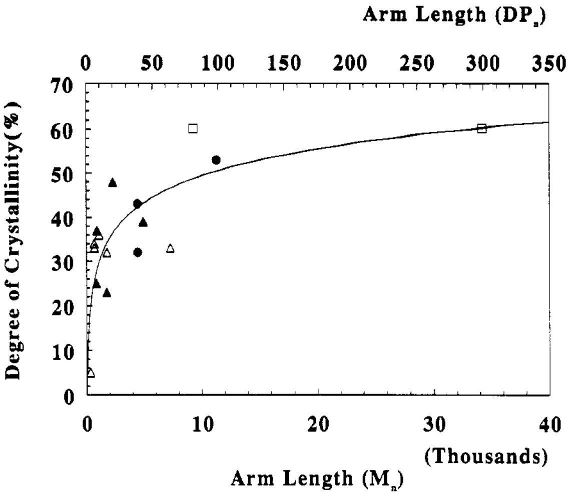

Figure 12. The effect of block size (arm length) on the degree of crystallinity of HPL–PCL starlike copolymers. Symbols are as in Figure 5.

HPL or by grafting preformed PCL segments onto HPL. Critical variables affecting copolymer properties are molecular weight of the arms (i.e., arm length) and number of arms per core. Both variables can be controlled during synthesis.

The intrinsic viscosity of the copolymers is a function of arm length, irrespective of the nature of the HPL. However, the synthesis method may have an effect on solution behavior of the copolymers. The grafting of PCL prepolymers onto HPL resulted in copolymers with higher intrinsic viscosity than the copolymers produced via anionic polymerization. The introduction of a strong polar group, such as TDI during the grafting process, may account for this increase.

The thermal behavior of the copolymers is somewhat affected by molecular weight. The copolymer melting point is the parameter that varies most with the length of the PCL arms. It approaches a limiting temperature (around 60 °C) as the copolymer arm length increases beyond 10000 D.

The crystallization of PCL chains is greatly affected by the T_g of HPL core. Starlike copolymers derived from HPL with T_g above room temperature require longer time to reach thermal equilibrium as compared to those copolymers synthesized from HPL with T_g below room temperature. This has a profound effect on the coarseness and shape of the spherulite morphology, which greatly depends on the "softness" of the HPL phase.

As expected, composition of the copolymer plays an important role in controlling the crystallization behavior of PCL chains. The degree of crystallinity of the copolymers is a function of arm length. The longer the arm length, the higher the degree of crystallinity.

Acknowledgment. Acknowledgement is made to Mr. Paul S. Vail for his technical assistance with the DSC experiments. The authors are also indebted to Dr. Abaneshwar Prasad for his skillful support with the optical microscopy measurements. This study was financially supported, in part, by a grant from the National Science Foundation (Contract No. 85/12636).

References and Notes

(1) Steinmann, H. W. *Polym. Prepr. (Am. Chem. Soc., Div. Polym. Chem.)* **1970**, *11*, 285.
(2) Feger, C.; Cantow, H.-J. *Polym. Bull.* **1980**, *3*, 407.
(3) Glasser, W. G.; Kelley, S. S. *Encycl. Polym. Sci. Eng.* **1987**, *8*, 795.
(4) de Oliveira, W.; Glasser, W. G. *J. Appl. Polym. Sci.* **1989**, *37*, 3119.
(5) de Oliveira, W.; Glasser, W. G. *ACS Symp. Ser.* **1989**, *No. 397*, 414.
(6) Kelley, S. S.; Rials, T. G.; Glasser, W. G. *J. Mater. Sci.* **1987**, *22*, 617.
(7) Kelley, S. S.; Glasser, W. G.; Wards, T. C. *J. Wood Chem. Technol.* **1988**, *8*, 341.
(8) Hofmann, K.; Glasser, W. G. *J. Wood Chem. Technol.* **1993**, *13* (1), 73.
(9) Huschen, J.; Jerome, J.; Teyssie, Ph. *Macromolecules* **1981**, *14*, 242.
(10) Koleske, J. V.; Roberts, R. M. J.; Gludice, F. P. U.S. Patent 3,670,045, June 13, 1972.
(11) Hsieh, H. L. *J. Appl. Polym. Sci.* **1978**, *22*, 1119.
(12) McGrath, J. E.; Hellstern, A. M.; DeSimone, J. M.; Long, T. E.; Cho, C.; Yoo, Y.; Wood, P.; DePorter, C. D.; Riffle, J. S. *Polym. Prepr. (Am. Chem. Soc., Div. Polym. Chem.)* **1988**, *29*, 57.
(13) Wu, L. C.; Glasser, W. G. *J. Appl. Polym. Sci.* **1984**, *29*, 1111.
(14) Glasser, W. G.; Barbero, A. M.; Zhang, S. Q.; McDaniel, K. Manuscript in preparation.
(15) Kelley, S. S.; Ward, T. C.; Rials, T. G.; Glasser, W. G. *J. Appl. Polym. Sci.* **1989**, *37*, 2961.
(16) Brink, A. E.; Sinai-Zingde, G.; Yoo, Y.; McGrath, J. E.; Riffle, J. S. *Polym. Prepr. (Am. Chem. Soc., Div. Polym. Chem.)* **1989**, *30* (1), 294.
(17) Frisch, K. C. In *Polyurethane Technology*; Bruins, P. F., Ed.; Interscience: New York, 1969; p 1.
(18) Tobolsky, A. V.; Rembaum, A. *J. Appl. Polym. Sci.* **1964**, *8*, 307.
(19) Siochi, E. S.; Ward, T. C.; Haney, M. A.; Mahn, B. *Macromolecules* **1990**, *23*, 1420.
(20) Haney, M. A. *J. Appl. Polym. Sci.* **1985**, *30*, 3023.
(21) Haney, M. A. *J. Appl. Polym. Sci.* **1985**, *30*, 3037.
(22) Chee, K. K. *J. Appl. Polym. Sci.* **1985**, *30*, 1323.
(23) Crescenzi, V.; Manzini, G.; Calzolari, G.; Borri, C. *Eur. Polym. J.* **1972**, *8*, 449.
(24) Salmén, L. *J. Mater. Sci.* **1984**, *19*, 3090.
(25) Candau, F.; Rempp, P.; Benoit, H. *Macromolecules* **1972**, *5*, 627.
(26) Bi, L. K.; Fetters, L. J. *Macromolecules* **1976**, *9*, 732.
(27) Huet, J. M.; Marechal, E. *Eur. Polym. J.* **1974**, *10*, 757.
(28) Perret, R.; Skoulios, A. *Makromol. Chem.* **1972**, *156*, 157.
(29) Bell, J. P.; Slade, P. E.; Dumbleton, J. H. *J. Polym. Sci.* **1968**, *A2* (6), 1773.
(30) Cheng, S. Z. D.; Cao, M.-Y.; Wunderlich, B. *Macromolecules* **1986**, *19*, 1868.
(31) Bassett, D. C.; Olley, R. H.; Al Raheil, I. A. M. *Polymer* **1988**, *29*, 1745.
(32) Marand, H.; Prasad, A. *Macromolecules* **1992**, *25*, 1731.
(33) Chatani, Y.; Okita, Y.; Tadokoro, H.; Yamashita, Y. *Polym. J. Jpn.* **1970**, *1*, 555.
(34) Heuschen, J.; Jerome, R.; Teyssie, Ph. *J. Polym. Sci.: Part B: Polym. Phys.* **1989**, *27*, 523.